ACS Chemical Neuroscience

pubs.acs.org/chemneuro

Research Article

In Vitro and In Silico Analysis of the Residence Time of Serotonin 5-HT$_7$ Receptor Ligands with Arylpiperazine Structure: A Structure−Kinetics Relationship Study

Eduardo Penna,[▽] Mauro Niso, Sabina Podlewska,[▽] Floriana Volpicelli, Marianna Crispino, Carla Perrone-Capano, Andrzej J. Bojarski, Enza Lacivita,* and Marcello Leopoldo

Cite This: https://doi.org/10.1021/acschemneuro.1c00710

Read Online

ABSTRACT: During the last decade, the kinetics of drug−target interaction has received increasing attention as an important pharmacological parameter in the drug development process. Several studies have suggested that the lipophilicity of a molecule can play an important role. To date, this aspect has been studied for several G protein-coupled receptors (GPCRs) ligands but not for the 5-HT$_7$ receptor (5-HT$_7$R), a GPCR proposed as a valid therapeutic target in neurodevelopmental and neuropsychiatric disorders associated with abnormal neuronal connectivity. In this study, we report on structure−kinetics relationships of a set of arylpiperazine-based 5-HT$_7$R ligands. We found that it is not the overall lipophilicity of the molecule that influences drug−target interaction kinetics but rather the position of polar groups within the molecule. Next, we performed a combination of molecular docking studies and molecular dynamics simulations to gain insights into structure−kinetics relationships. These studies did not suggest specific contact patterns between the ligands and the receptor-binding site as determinants for compounds kinetics. Finally, we compared the abilities of two 5-HT$_7$R agonists with similar receptor-binding affinities and different residence times to stimulate the 5-HT$_7$R-mediated neurite outgrowth in mouse neuronal primary cultures and found that the compounds induced the effect with different timing. This study provides the first insights into the binding kinetics of arylpiperazine-based 5-HT$_7$R ligands that can be helpful to design new 5-HT$_7$R ligands with fine-tuning of the kinetic profile.

KEYWORDS: *residence time, lipophilicity, serotonin receptor 7, arylpiperazines, neurite elongation*

■ INTRODUCTION

Over the years, the affinity and the potency of a drug candidate for a given target measured at the equilibrium have been the sole parameters to guide the process of drug discovery. In recent years, the temporal aspects of drug−receptor interactions are receiving growing interest. The association rate of a drug with its receptor (k_{on}) may be just as important as the length of time the drug is bound (residence time, $1/k_{off}$) in determining drug pharmacodynamics in vivo.[1,2] The association rate is considered an important factor in determining the drug activity profile. As an example, slowly associating drugs may have lower on-target related side effects by preventing high receptor occupancy and fast activation,[3] while fast-associating drugs may prolong activity if rebinding takes place.[4] The residence time of a drug is currently discussed as one of the most important contributors to the biological efficacy of drugs *in vivo*.[1,2,5] It has been postulated that a suitably long residence time might increase the therapeutic window in vivo if the drug is cleared faster than it dissociates from the receptor.[6,7] The preference for drugs with "long" or "short" residence time may vary for different targets or different therapeutic indications.[8] Long-residence-time drugs offer advantages for those therapies requiring prolonged target occupancy so that the drug continues to exert its pharmacological effect even when most of the free drug has

Received: October 28, 2021
Accepted: January 19, 2022

Table 1. Equilibrium and Kinetic Binding Parameters of Reference Compounds

Compd		Equilibrium K_i ± SEM (nM)	k_{on} ± SEM (M^{-1}, min^{-1})	k_{off} ± SEM (min^{-1})	Kinetically derived $K_d = k_{off}/k_{on}$ ± SEM (nM)	RT = $1/k_{off}$ ± SEM (min)
[^{3}H]-5-CT		0.20 ± 0.05	(9.350±3.12)×10^7	0.01679±0.0061	0.18 ± 0.06	59 ± 13
5-CT	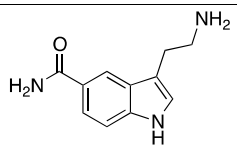	0.43 ± 0.13	(3.140±1.13)×10^7	0.01976±0.0059	0.63 ± 0.17	50 ± 12
5-HT	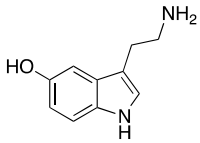	1.20 ± 0.31	(2.364±0.12)×10^8	0.2759±0.0138	1.16 ± 0.40	3.6 ± 0.2
LP-211	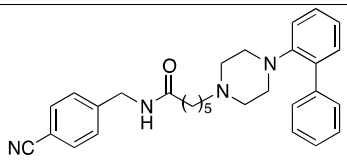	20.0 ± 3.2	(1.744±0.23)×10^6	0.04157±0.0051	23.8 ± 4.2	24.0 ± 2.9
SB-269970	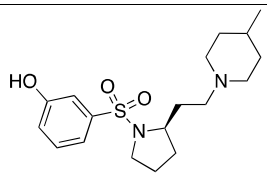	3.50 ± 0.81	(2.641±0.70)×10^7	0.08221±0.0205	3.11 ± 0.78	12.0 ± 3.1

already been eliminated from circulation.[9] One example is the muscarinic M_3 receptor antagonist tiotropium (dissociation half-life = 27 h), a long-acting bronchodilator used to manage the chronic obstructive pulmonary disease.[10] On the other hand, long receptor occupancy can be related to mechanism-based toxicity and, thus, a fast-dissociating drug is preferred. This may be the case with the antipsychotic dopamine D_2 antagonists, for which long residence times are associated with severe extrapyramidal motor effects.[11]

Thus, considering the binding kinetics as an additional parameter in the process of lead-compound selection and optimization can decrease the attrition rate of the drug development process and lead to the identification of clinical candidates with optimal in vivo efficacy.[1,2,12] This is particularly relevant for drugs targeting G protein-coupled receptors (GPCRs), representing about 33% of all small-molecule drugs.[13]

Serotonin receptor type 7 (5-HT_7R) is a class A GPCR and is the most recently discovered serotonin receptor subtype. 5-HT_7R is involved in numerous physiological functions including thermoregulation, sleep regulation and circadian rhythm, learning and memory, synaptic plasticity, mood control, and nociception.[14] 5-HT_7R blockade has antidepressant effects and may ameliorate cognitive deficits associated with schizophrenia.[15] Recent studies have demonstrated that 5-HT_7R modulates neuronal morphology, excitability, and plasticity, thus contributing to shaping brain networks during the development and remodeling of neuronal connectivity in the fully developed adult brain.[16−19] Therefore, 5-HT_7R activation has been proposed as a valid therapeutic approach for neurodevelopmental and neuropsychiatric disorders associated with abnormal neuronal connectivity.[20−23]

Considering the potential therapeutic role of 5-HT_7R agents and the increasing importance of drug−receptor kinetic binding parameters for the development of next-generation drugs, we carried out the investigation of the binding kinetics of a set of 5-HT_7R ligands and in silico studies to identify the ligand/binding site interactions that might influence the residence time. Finally, we evaluated if residence time could impact the biological activity by comparing the effects of the reference 5-HT_7R agonist LP-211[24] (residence time = 24 min, Table 1) with the novel agonist **4** characterized by a lower residence time (8.7 min, Table 2) on 5-HT_7R-mediated neurite outgrowth in mouse primary neuronal cultures. To the best of our knowledge, the structure−kinetics relationships (SKRs) of 5-HT_7R ligands have never been studied so far, as well as the influence of the kinetics of ligand-5-HT_7R interaction on the biological activity.

RESULTS AND DISCUSSION

Binding Kinetics: Initial Setting. Binding kinetics at a GPCR can be assessed using different methodologies, which include radioligand binding assay and fluorescence-based methods.[25] In this study, radioligand binding assays were performed using [^{3}H]-5-CT, an agonist radioligand commonly used to assess 5-HT_7R affinity, and membrane preparations from HEK-293 cell stably transfected with human 5-HT_7R. Initial experiments were aimed at complete characterization of [^{3}H]-5-CT binding kinetic parameters because incomplete data were available or different experimental protocols have been used.[26,27] [^{3}H]-5-CT equilibrium and kinetic parameters are reported in Table 1. The determination of k_{off} was assessed by prelabeling of 5-HT_7R with a [^{3}H]-5-CT concentration (approximately 10 × K_d) able to provide high initial receptor occupancy. Then, the radioligand dissociation was induced by adding a saturating concentration of unlabeled 5-CT (approximately 1000 × K_d). The k_{on} value was obtained from the association curve (Figure 1) as detailed in the

https://doi.org/10.1021/acschemneuro.1c00710
ACS Chem. Neurosci. XXXX, XXX, XXX−XXX

Table 2. Equilibrium and Kinetic Binding Parameters of the Selected Set of 5-HT$_7$R Ligands[abc]

Compd		ClogD$_{7.4}$[a]	log*k'*	Equilibrium K_i ± SEM (nM)	k_{on} ± SEM (M^{-1}, min^{-1})	k_{off} ± SEM (min^{-1})	Kinetically derived K_d= k_{off}/k_{on} ± SEM (nM)	RT = 1/k_{off} ± SEM (min)
1	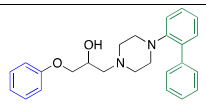	4.13	1.09	1.31 ± 0.20[b]	(1.817±0.06) ×10^7	0.02154±0.0073	1.18 ± 0.30	46.0 ±15.2
2	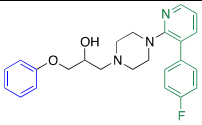	3.81	0.82	47.5 ± 3.5	(2.764±0.64) ×10^6	0.1405±0.0285	50.8 ± 4.5	7.0 ±1.4
3	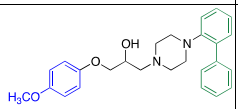	3.99	0.97	15.0 ± 1.8	(2.417±0.33)×10^6	0.03235±0.0045	13.4 ± 2.1	31.0 ±4.3
4	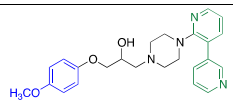	2.30	-0.03	19.3 ± 1.1[b]	(4.708±1.23) ×10^6	0.1145±0.0274	24.3 ± 3.1	8.7 ± 2.1
5	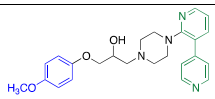	2.29	0.06	22.1 ± 0.1[b]	(4.581±0.91) ×10^6	0.1178±0.0234	25.7 ± 1.1	8.5 ± 1.7
6	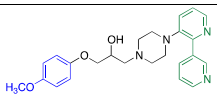	2.03	-0.06	57.0 ± 1.7[b]	(4.592±0.95) ×10^5	0.03012±0.0084	65.6 ± 3.8	33.0 ± 9.2
7	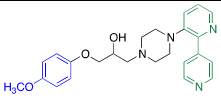	2.09	-0.10	16.8 ± 3.5[b]	(2.804±0.25) ×10^6	0.06997±0.0282	24.9 ± 1.7	16.0 ± 9.3
8	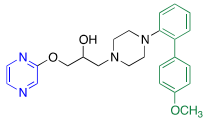	2.28	0.70	1.10 ± 0.30[b]	(3.984±0.43) ×10^7	0.05045±0.0027	1.27 ± 0.30	19.8 ± 1.1
9	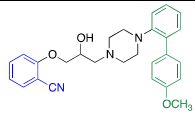	3.88	0.90	17.7 ± 5.0[c]	(1.878±0.24) ×10^6	0.03343±0.0011	17.8 ± 2.5	30.0 ± 0.9
10	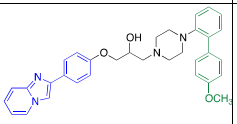	4.0	1.02	25.7 ± 2.6[c]	(1.491±0.24) ×10^6	0.04379±0.0150	29.4 ± 5.1	22.8 ± 7.7
11	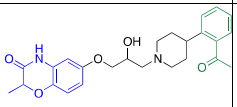	1.78	0.18	46.7 ± 3.7	(1.759±0.08) ×10^6	0.07455±0.0160	42.4 ± 6.2	13.0 ± 2.7
12	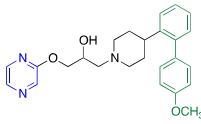	1.87	0.04	15.2 ± 1.4[c]	(1.545±0.54) ×10^6	0.02915±0.0093	18.9 ± 2.3	34.0 ± 1.1

[a]Calculated with ChemAxon Software (Instant JChem 15.3.30.0, ChemAxon, 2015. http://www.chemaxon.com). [b]Data taken from ref 33. [c]Data taken from ref 34.

https://doi.org/10.1021/acschemneuro.1c00710
ACS Chem. Neurosci. XXXX, XXX, XXX−XXX

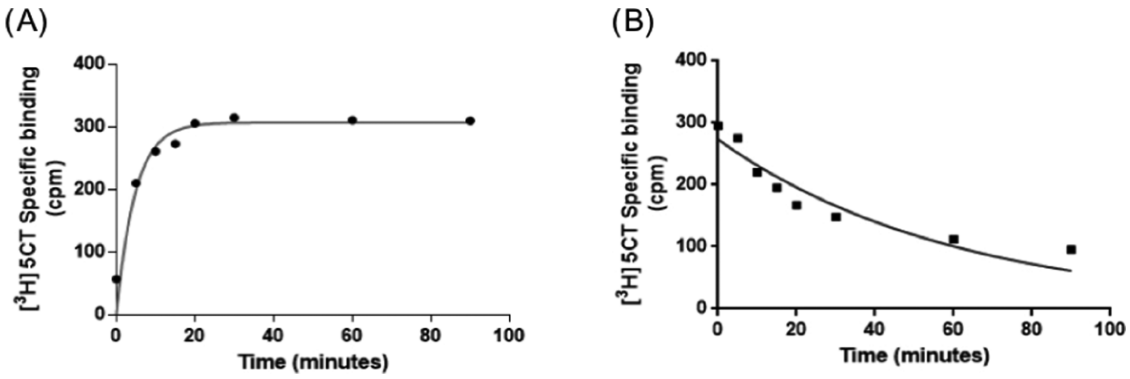

Figure 1. (A) [^{3}H]-5-CT binding association kinetics; (B) [^{3}H]-5-CT binding dissociation kinetics

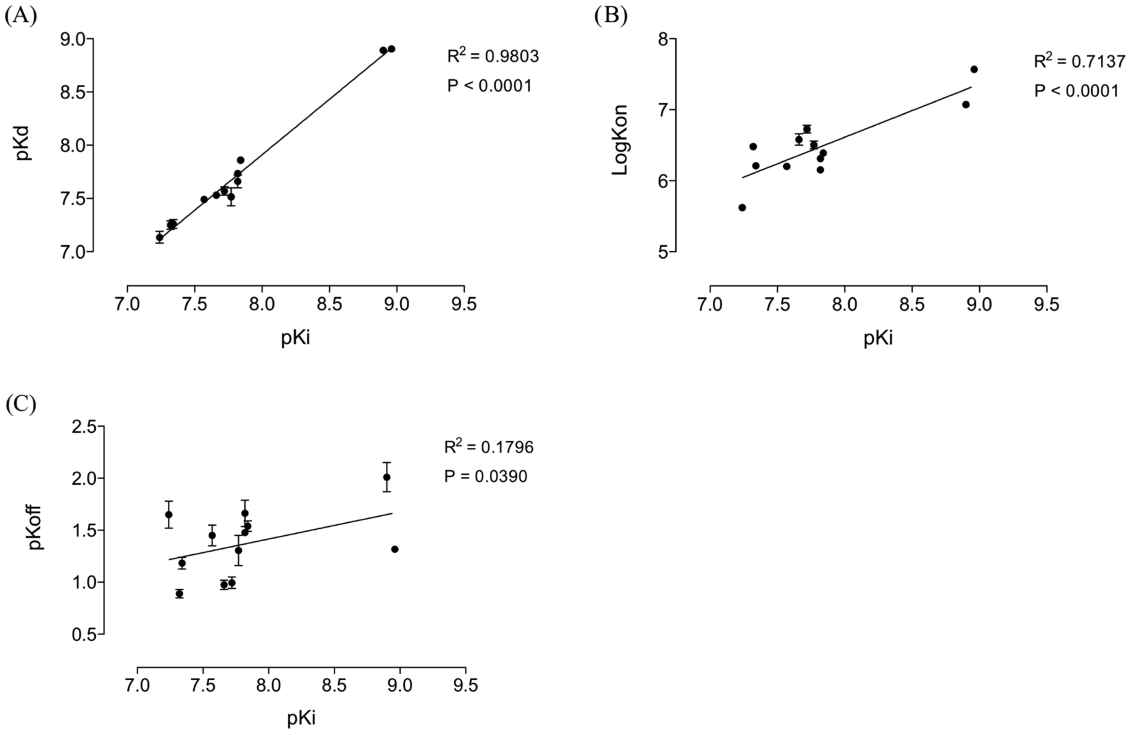

Figure 2. Comparison between equilibrium binding affinity and binding kinetics. Correlation plots of equilibrium affinity (pK_i) with the negative logarithmic transformation of kinetic affinity (pK_d) (A), association rate k_{on} (B), and dissociation rate k_{off} (C).

Experimental Section. The kinetically derived K_d for [^{3}H]-5-CT (kinetic $K_d = k_{off}/k_{on}$, 0.18 nM) was in good agreement with the K_d obtained from saturation experiments (K_d = 0.20 nM) (Table 1).

Binding Kinetics of 5-HT$_7$R Ligands. Once the k_{on} and k_{off} of [^{3}H]-5-CT are determined, the kinetic parameters of the unlabeled compounds were assessed (Tables 1 and 2). In brief, a concentration of the unlabeled competitor (approximately 10 × K_i) was added simultaneously with the radioligand to the receptor and the experimentally derived rate of specific radioligand binding was analyzed using the equations developed by Motulsky and Mahan.[28] This approach allowed us to determine the association and dissociation rates of each unlabeled compound (k_{on} and k_{off}) that were used to calculate kinetic K_d and residence time (Tables 1 and 2). Considering the paucity of data in the literature on the binding kinetics of 5-HT$_7$R ligands, we assessed the kinetic parameters of several 5-HT$_7$R reference agonists and antagonists (Table 1). All compounds showed faster dissociation kinetics than the radioligand; therefore, the time required to reach the equilibrium for "on-rate" and "off-rate" experiments as well as the radioligand concentration were adequately selected to have a proper assessment of the kinetic parameters of the unlabeled compounds.[28]

Next, we selected a set of arylpiperazine-based 5-HT$_7$R ligands characterized by the general formula Ar−piperazine−aryloxypropanol linker−terminal fragment from our in-house library. It has been proposed that the general physicochemical properties of a ligand, such as lipophilicity or rotational bonds, may affect the residence time and that modulating such properties can lead to "fine-tuned drug−target binding kinetics".[29−32] Thus, to address this aspect, we selected a set of compounds covering a wide range of lipophilicity (expressed as $c\log D_{7.4}$), from $c\log D_{7.4}$ = 4.13 for the most lipophilic compound (**1**) to $c\log D_{7.4}$ = 1.78 for the less lipophilic compound (**11**).[33,34] The set also included 5-HT$_7$R ligands having similar $c\log D_{7.4}$ values but variable lipophilicity of their Ar group or terminal fragment. Thus, we assessed the binding

https://doi.org/10.1021/acschemneuro.1c00710
ACS Chem. Neurosci. XXXX, XXX, XXX−XXX

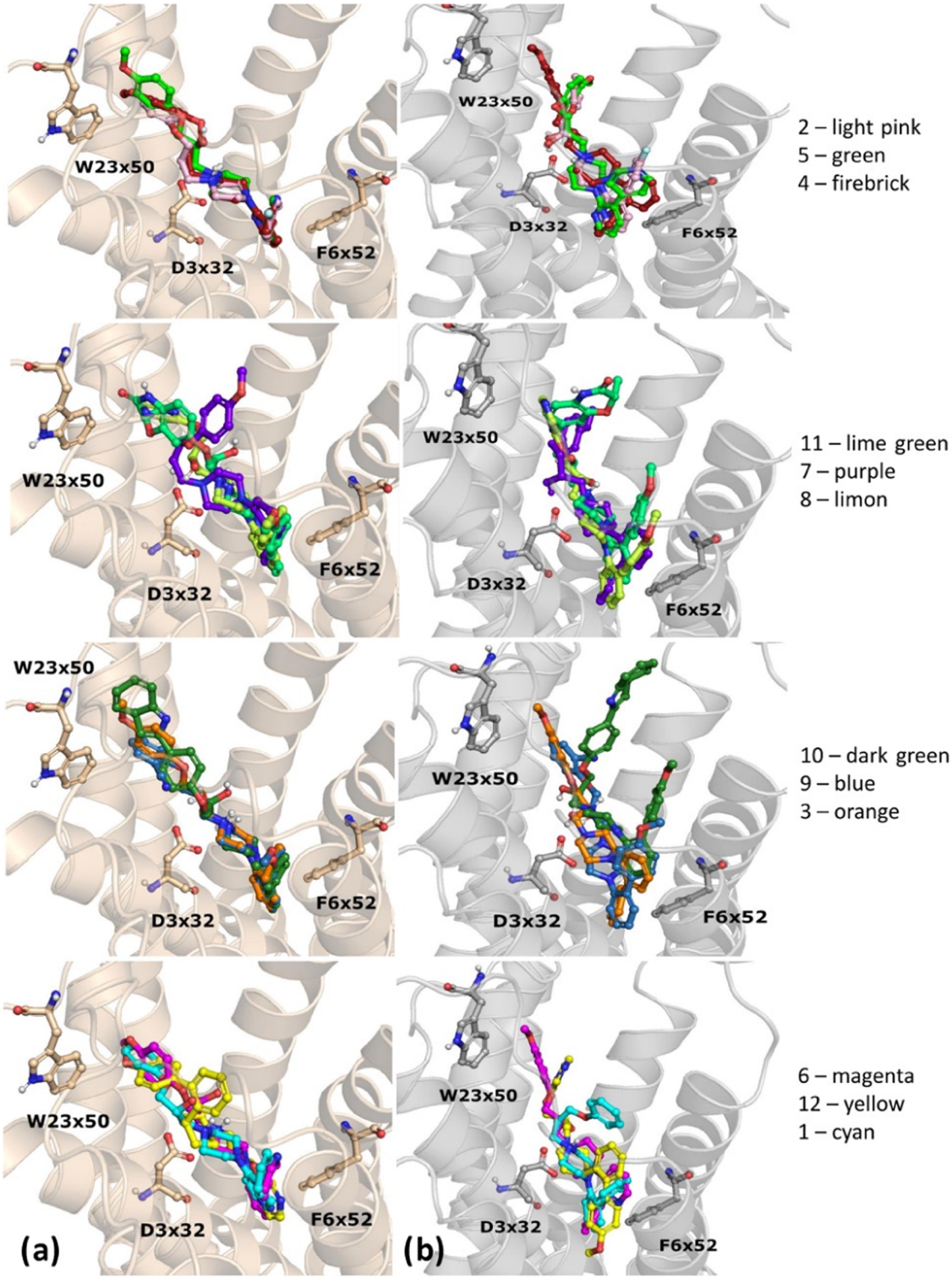

Figure 3. Analysis of docking poses of the studied compounds to the active (a) and inactive (b) forms of 5-HT7R.

kinetic parameters of compounds **1**−**12** to evaluate if the overall lipophilicity of the molecule or the lipophilicity of a specific fragment influences the kinetics of drug−receptor interaction (Table 2).

The kinetic K_d's of all compounds were then compared to the equilibrium affinities (K_i). A statistically significant correlation was found between the negative logarithm of the kinetic K_d (pK_d) and the equilibrium pK_i, indicating that the method produced accurate k_{on} and k_{off} rates (Figure 2A). Moreover, a linear correlation between pK_d and k_{on} was also identified (Figure 2B) but not between pK_d and k_{off} (Figure 2C), suggesting that the binding affinity was influenced mainly by the association rate rather than the dissociation one, as reported for other receptor GPCRs.[35−37]

The kinetic profile of the compounds enabled the description of the SKRs. The highest residence time was shown by compound **1**, which was also the most lipophilic compound of the series. The lowest residence times were

https://doi.org/10.1021/acschemneuro.1c00710
ACS Chem. Neurosci. XXXX, XXX, XXX−XXX

shown by compounds **2**, **4**, and **5**. Of note, compounds **4** and **5** have very similar lipophilicity (and residence time), whereas compound **2** has a clogD$_{7.4}$ value 1.5 log units higher than **4** and **5**. This clearly suggests that the overall lipophilicity of the molecule is not the main property that influences the residence time. Indeed, no correlation was found between the k_{on}, k_{off}, or residence time and clogD$_{7.4}$ values (data not shown). We also assessed the chromatographic retention index (log k') as a lipophilicity index of the molecule. Also in this case, we did not find any correlation between residence time and log k' (see Supporting Information Figure S1B). Comparing compounds **4** and **5** (featuring a 2-pyridyl group linked to the piperazine ring) with the corresponding 3-pyridyl isomers **6** and **7**, it can be noted that the simple formal shifting of the pyridine aza group has an effect on the residence time. In fact, the residence times of **6** and **7** are 4- and 2-fold higher than the residence times of compounds **4** and **5**, respectively. These data suggest that the position of the polar aza group in the biphenyl-like system linked to the piperazine ring has a relevant role in the kinetics of ligand-5-HT$_7$R interaction.

Compounds **3**, **8**, **9**, **10**, and **12**, which have no polar groups on the biphenyl system and present terminal groups characterized by different lipophilic properties, had residence times higher than 20 min. These data confirmed that the overall lipophilicity of the molecule was not correlated with the residence times. In fact, compounds **3** and **12** showed very similar residence time and 2-units difference in c log D$_{7.4}$ value.

Finally, we tested compound **11**, which features the 2-acetylphenyl ring linked to the piperazine ring instead of the 4-methoxybiphenyl system. We found that the residence time of **11** was close to that of compounds **4** and **5**. Although compound **11** is the only example with the aryl substituent different from the biphenyl/bipyridyl, the observed residence time suggests that the lipophilicity of the ring system linked to the piperazine ring can have a role in the residence time of this group of compounds. In fact, the variation 2-acetylphenyl/4-methoxybiphenyl implies a reduction of lipophilicity (ΔC log D7.4 = 1.56) that is similar to that of the variation bipyridyl/4-methoxybiphenyl (ΔC log D7.4 = 1.53).

Collectively, the data suggest that the lipophilicity of the "right-hand-side" part compared to the "left-hand-side" part of the molecule has a more significant impact on the kinetics of the interaction between the ligand and 5-HT$_7$R. In addition, the data suggest that the position of polar groups in the right-hand-side part of the molecule impacts the residence time.

Computational Studies. Several studies have attempted to identify the structural features of a ligand that influence the kinetic parameters, but drawing SKRs was not straightforward.[38] While other studies have indicated lipophilicity as one of the most important properties that affect residence time,[32] we did not find any correlation between the overall lipophilicity of the molecule and the kinetic parameters. Thus, we attempted to correlate the residence time with several molecular descriptors, but the obtained R^2 values did not indicate any significant correlation (see Supporting Information Figure S2).

Several in silico approaches and methodologies, characterized by different complexity and computational demands, have been reported in the literature as a support in the prediction of compound kinetics. The most straightforward approaches use docking and analyze the outcomes qualitatively[39] or quantitatively.[40−43] More complex but more accurate are kinetics predictions based on molecular dynamics (MD) simulations. Although the timescales of compound dissociation are much longer than the current available time for typical MD (minutes to hours vs μs), there are several approaches to simulate long-time events from short trajectories. This problem has been tackled, e.g., by running a large number of short trajectories in parallel,[44,45] applying an external force to induce the occurrence of rare events,[46] or increasing the temperature of the system so that the energy barrier can be crossed more easily.[47]

In this study, we combined docking and MD simulations to draw the SKRs of the studied 5-HT$_7$R ligands. The results were examined qualitatively focusing on the stability of the compound pose in the binding site. Compounds were docked to a homology model of 5-HT$_7$R in the active or inactive conformation. The homology model of the inactive conformation was constructed according to a previously described procedure,[48] whereas the active conformation was fetched from the GPCRdb repository.[49] We found that the orientations of compounds in the binding pocket were analogous for both receptor conformations, with the piperazine moiety forming a strong charge-assisted hydrogen bond with D3 × 32 and the biphenyl/bipyridyl moiety being deeply buried into the binding site (Figure 3). In addition, to facilitate the interpretation of the results and the detection of differences in the interaction patterns occurring for the studied compounds, the contacts formed by ligands in the 5-HT$_7$R binding site are presented in the form of ligand−protein interaction matrices (see Supporting Information Figure S3).

These poses were obtained using a standard docking procedure for most compounds. Only for compound **8**, an induced-fit docking (IFD) procedure was applied to enable such ligand fitting. As the docking outcome constitutes the input for MD simulations, the IFD was used to model compound **8** fitting in the binding site to provide consistency in the initial orientation of all studied compounds.

More detailed analysis of docking studies supported by the use of ligand-interaction matrix revealed that there is a relatively extended set of interactions that consistently occur for all of the analyzed compounds (D3 × 32, V3 × 33, T3 × 37, F6 × 51, F6 × 52, and R7 × 35 for active 5-HT$_7$R and D3 × 32 and Y7 × 42 for the inactive receptor form). On the other hand, some contacts occur specifically for some ligands; however, they are not correlated to the compound residence time.

Since there are indications in the literature that the interaction of a ligand with the extracellular vestibule of the receptor (often referred to as the secondary binding pocket, SBP) can influence the binding kinetics,[39] we examined the interactions of compounds **3**−**7** (that feature the same terminal fragment) and **8**−**10** (that feature the same arylpiperazine moiety) to highlight the contribution of the extension of the molecule from the inner part of the binding pocket toward the SBP on the observed residence time of the compounds. No correlation was found between the interaction contacts of the two parts of the molecules (i.e., the terminal fragment or the arylpiperazine moiety) and the residence time (see Supporting Information Figure S4).

As docking did not provide any clear relationship between the ligand−protein contacts and compounds' residence time, MD simulations were used as a qualitative supplement to the docking studies. MD simulations were performed for all of the studied compounds using the inactive form of the receptor. Confirmative studies were performed using the active form of

https://doi.org/10.1021/acschemneuro.1c00710
ACS Chem. Neurosci. XXXX, XXX, XXX−XXX

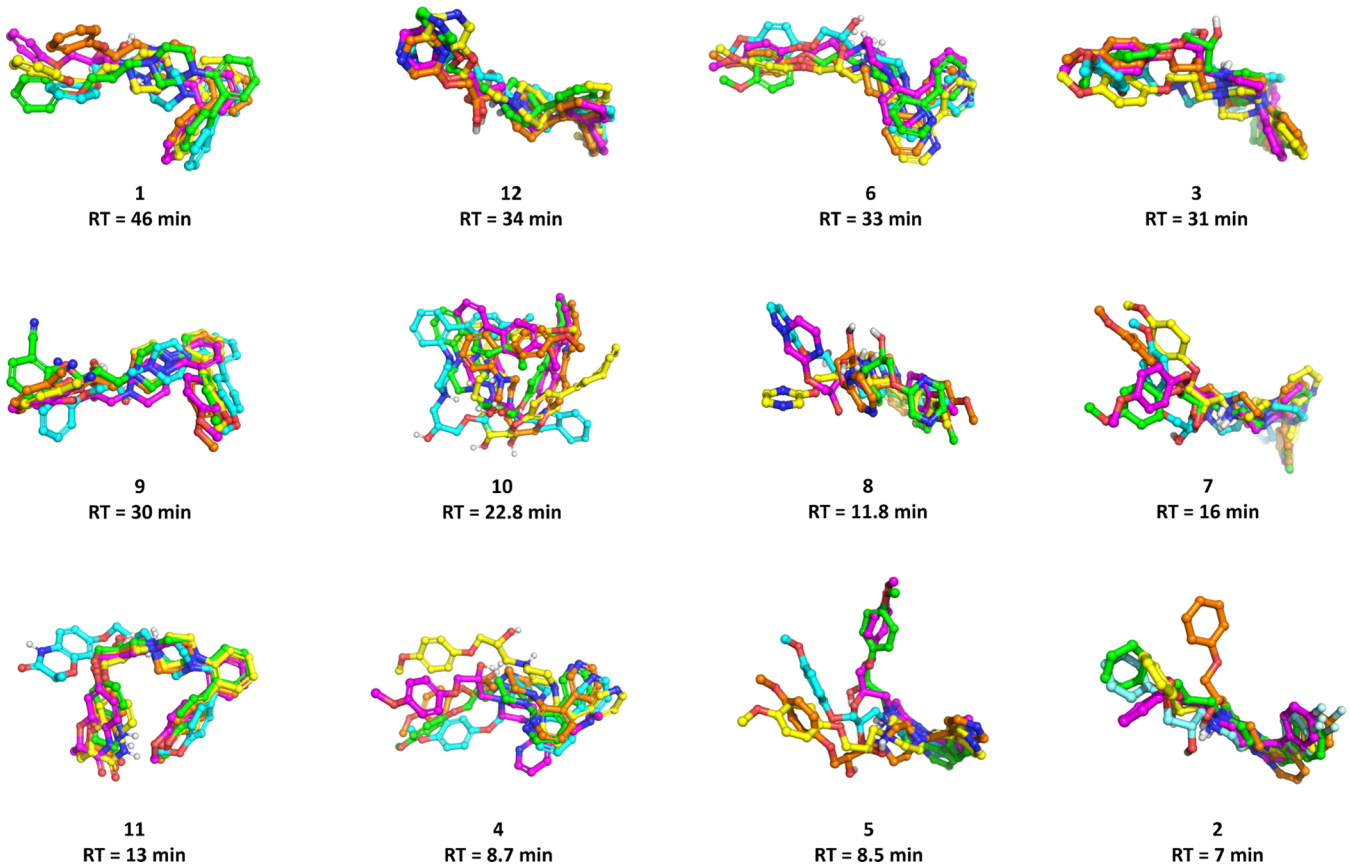

Figure 4. Comparison of ligand poses during MD simulation of the studied compounds with the inactive form of 5-HT$_7$R (cyan: starting pose; yellow: after 250 ns; orange: after 500 ns; magenta: after 750 ns; green: after 1000 ns)

the receptor on a subset of the studied compounds (see Supporting Information Figure S5). To examine the stability of modeled ligands in the binding site, five compound conformations (starting pose and four other poses captured at 250, 500, 750, and 1000 ns of simulation) were analyzed (Figure 4). In addition, to examine ligand stability more formally, the root-mean-square deviation (RMSD) was monitored (see Supporting Information S6) and the Pearson correlation coefficient between the average RMSD and compound residence time was determined (Figure 5). The Pearson correlation coefficient showed a value of −0.552 that indicates a strong correlation between the examined compound properties. Moreover, Figure 5 indicates that, in general, compounds characterized by higher residence time are more stably fitted in the 5-HT$_7$R binding site during MD, which is expressed by lower RMSD values. Analysis of compound poses at different time points of MD simulations (Figure 4) confirms the "compound stability theory" with reference to its binding kinetics.

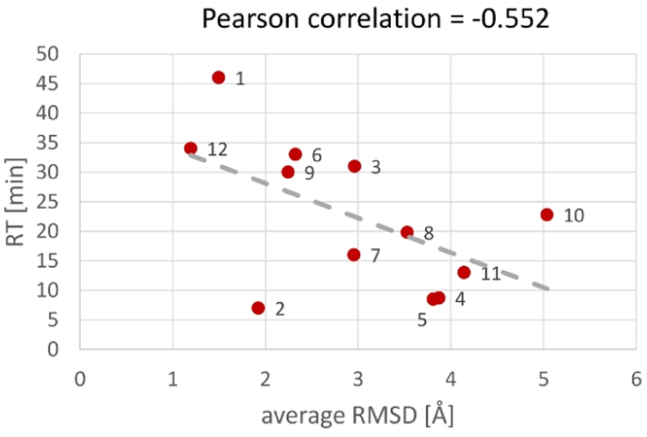

Figure 5. Relationship between the residence times and average RMSD of compounds during MD.

Interestingly, in most cases, the compound flexibility was connected with the variation of the orientation of the aryloxy moiety. Except for compound **10**, the piperazine and biphenyl/bipyridyl moieties are always stably fitted in the binding site, mainly as a result of a strong charged-assisted interaction of the protonated basic nitrogen with D3 × 32. Compounds **1**, **3**, **6**, **9**, and **12**, which had residence times of 30 min or higher, adopted very similar orientations during MD simulations. Instead, a high variability of atom positions during MD simulation was observed for compound **10** (residence time = 22.8 min), with a tendency for the compound to egress the 5-HT$_7$R binding site slightly faster than other compounds with a similar residence time. A possible explanation of this could be the higher steric hindrance of the terminal fragment of compound **10** that did allow us to reach a stable conformation. Compounds **2**, **4**, **5**, **7**, **8**, and **11**, which had residence times below 12 min and egressed from the receptor-binding site faster, stably fitted their piperazine and biphenyl/bipyridyl moieties within the binding pocket. At the same time, conformational variations were observed mainly in the terminal fragment. A detailed analysis of all MD poses in the form of

https://doi.org/10.1021/acschemneuro.1c00710
ACS Chem. Neurosci. XXXX, XXX, XXX−XXX

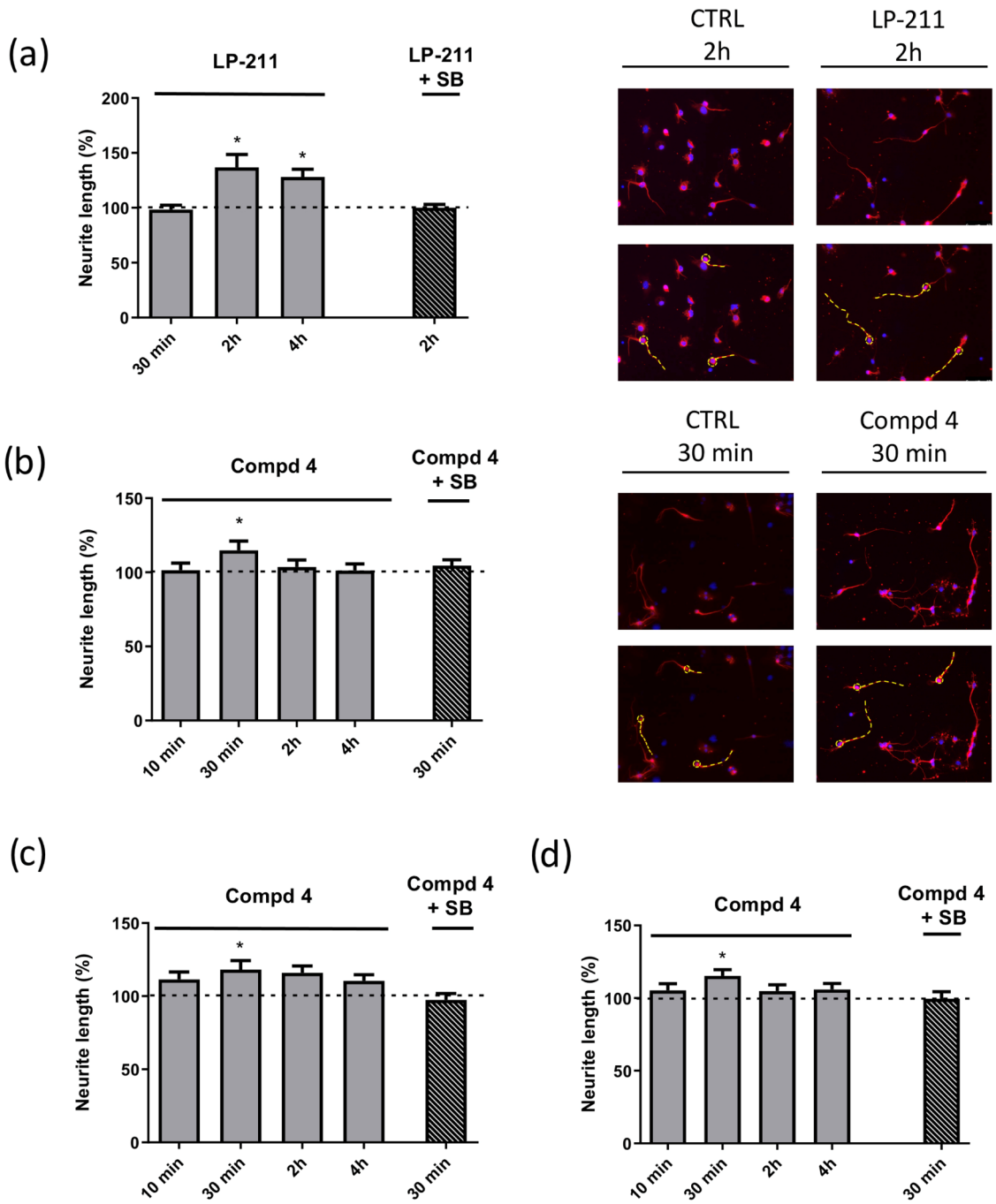

Figure 6. 5-HT$_7$R agonists stimulate neurite outgrowth in primary neuronal cultures. Striatal primary neurons from P1−P3 mice were treated with (a) LP-211 (100 nM) or (b) compound **4** (100 nM) at different time points alone or in the presence of the selective 5-HT$_7$R antagonist SB-269970 (100 nM). The panels on the right display representative images of control (CTRL) and drug-treated neurons immunostained with the neuronal marker Tuj1 (red) and counterstained with the nuclear marker DAPI (blue; magnification 20×). The dashed yellow lines were manually drawn by the operator from the soma (yellow circle) to the end of the primary neurite to measure neurite length. (c) Cortical and (d) hippocampal primary neurons treated with compound **4** (100 nM) at different time points. Neurite length was measured on cells stained with anti-Tuj1 antibody and expressed as the percentage of the values measured in the corresponding vehicle-treated cultures (CTRL, set to 100%, dashed line). The bars represent standard error of mean (SEM) from randomly selected fields for each cell culture condition (n = 4). * Significantly different from CTRL by Student's t-test ($p < 0.05$).

ligand−protein interaction matrices is available in the Supporting Information (Figure S7).

Finally, we evaluated if the extracellular loops impact the residence time of our compounds. Several studies have reported that extracellular loop 1 (ECL1) or ECL2 can function as a "lid" over the binding pocket, thereby modulating the entrance or the egress of a ligand from the binding site. In particular, specific amino acid residues have been identified as crucial for the interaction with the ligand.[50−53] As an example, Wacker et al. identified the hydrophobic residue L209 in ECL2 of the 5-HT$_{2B}$ receptor as a key residue for the residence time of LSD.[50] Similarly, W100 in the ECL1 of dopamine D$_2$ receptor was reported as a crucial amino acid residue influencing the residence time of several dopamine D$_2$

https://doi.org/10.1021/acschemneuro.1c00710
ACS Chem. Neurosci. XXXX, XXX, XXX−XXX

antagonists.[52,53] As both amino acid residues are relatively well conserved in aminergic receptors, we examined both the positions of W23 × 50 and ECL2 residues, as well as their interaction with modeled ligands. However, although the lid formation was observed, no correlation between the ECL1 and ECL2 amino acids position in MD simulations for different compounds and residence time was observed. Similarly, no correlation between compound interactions with ECL1/ECL2 and ligand kinetics was identified. A detailed analysis of the W23 × 50 position and interaction patterns of modeled ligands with 5-HT$_7$R ECL1/ECL2 residues during MD is available in the Supporting Information (Figures S8−S11).

Summing up, docking studies did not suggest specific contact patterns between the ligands and the receptor-binding site as determinants for the kinetics of the compounds. Nonetheless, we noted a tendency of stable poses of the compounds with a longer residence time in the binding pocket throughout the MD simulations. Instead, fast conformational changes noted for ligands with shorter residence times are likely to facilitate the ligand egress from the binding site.

Neurite Outgrowth Studies. We previously reported that pharmacological stimulation of 5-HT$_7$R with the selective agonist LP-211 in rodent neurons in culture significantly increased neurite outgrowth compared to the vehicle-treated control cultures.[17−19] An interesting aspect of LP-211 action was that its effect started after 2 h of stimulation and was still present after 4 h, then progressively diminished over time.[17−19,54] This effect was 5-HT$_7$R-specific, as no effect on neurite elongation was observed in neurons treated with LP-211 and the selective 5-HT$_7$R antagonist SB-269970.

The analysis of the arylpiperazine derivatives reported in Table 1 led to the identification of compounds **2**, **4**, and **5** that have residence times close to 8 min, i.e., 3-fold lower than LP-211, which has a residence time of 24 min. Thus, in an initial attempt to correlate the residence time with biological activity, we selected compound **4**, which showed the K_i value very close to LP-211 and evaluated the effect on neurite elongation compared to LP-211. After 3 days in culture, primary neuronal cultures dissociated from hippocampus, cortex, and striatum of postnatal day 1 (P1) or 3 (P3) mice were stimulated for 10 min, 30 min, 2 h, and 4 h with compound **4** with or without the selective 5-HT$_7$R antagonist SB-269970 (Figure 6). The stimulation of striatal cultures with 100 nM compound **4** induced a time-dependent increase in neurite length compared to control with a peak at 30 min (about 15%, Figure 6B). Indeed, although at 2 h, the neurite length appeared still higher than control, the value was not statistically significant. We obtained similar results also in cortical and hippocampal neurons (Figure 6C,D). This morphogenic effect was completely abolished when compound **4** was incubated in the presence of SB-269970 (Figure 6B), demonstrating that the increased neurite length was specifically due to the selective stimulation of 5-HT$_7$R by compound **4**. Thus, the effect of compound **4** displays a different timing compared to LP-211 as it starts much earlier (30 min) and ends rapidly (Figure 6).

■ CONCLUSIONS

In summary, we have reported the SKRs of a set of arylpiperazine-based 5-HT$_7$R ligands. We found that the lipophilicity of the aryl moiety linked to the piperazine ring has a more significant impact on the kinetics of binding than the lipophilicity of the terminal fragment attached to the alkyl chain. In addition, the position of polar groups on the aryl moiety linked to the piperazine ring impacts the residence time.

Molecular docking and MD simulation studies did not point to specific contacts between the ligands and the binding site that might be responsible for the observed residence time of the compounds. Yet, MD simulations evidenced a tendency of stable poses in the binding site of the compounds with longer residence times, differently from the compounds with shorter residence times whose fast conformational changes are likely to ease the egress of the ligand from the binding site. With this respect, the availability of the crystal structure of 5-HT$_7$ receptor would be of paramount importance to evidence possible water molecules assisting the ligand−protein interaction, as it was reported for crystallized GPCRs.[39]

Finally, we found that the 5-HT$_7$R agonist **4** (residence time = 8.7 min) induced neurite elongation in primary neuronal cultures from different brain areas with different timing compared to the reference 5-HT$_7$R agonist LP-211(residence time = 24 min). This experiment is far beyond to be conclusive regarding the correlation between the binding kinetics and subsequent cellular events. Yet, we believe that our findings can be of inspiration for further focused investigations.

This study provides the first insights into the binding kinetics of arylpiperazine-based 5-HT$_7$R ligands. The results of this study can be helpful to design new 5-HT$_7$R ligands with fine-tuning of the kinetic profile, which could support the optimization process of new 5-HT$_7$R agonists for the treatment of neurodevelopmental disorders. In addition, this study provides further information regarding the structural features that influence the binding kinetic properties of arylpiperazine derivatives, which are known to bind to serotonin, dopamine, and adrenergic receptors.

■ METHODS

Chemistry. The studied compounds have been prepared as previously reported[33,34] or as detailed in the Supporting Information.

Radioligand Binding Assays. *Materials.* HEK-293−5HT$_{7A}$ transfected cell line was developed in our laboratory as previously reported.[55] Cell culture reagents were purchased from EuroClone (Milan, Italy). G418 (geneticin) and 5-HT were purchased from Sigma-Aldrich (Milano, Italy). 5-CT and SB-269970 were purchased from Tocris Bioscience (Bristol, U.K.). [^{3}H]-5CT was obtained from PerkinElmer Life and Analytical Sciences (Boston, MA). MultiScreen plates with glass fiber filters were purchased from Merck Millipore (Billerica, MA).

Cell Culture. HEK-293−5-HT$_{7A}$ transfected cells were grown in high-glucose DMEM supplemented with 10% fetal bovine serum, 2 mM glutamine, 100 U/mL penicillin, 100 μg/mL streptomycin, and 0.1 μg/mL G418 in a humidified incubator at 37 °C with a 5% CO_2 atmosphere.

Competition Binding Assay. 5-HT$_7$R competition binding assay was carried out as previously reported.[55] The experiments were performed in MultiScreen plates (Merck Millipore) with glass fiber filters (GF/C), presoaked in 0.3% poly(ethylenimine) for 20 min. After this time, 130 μg of HEK-293−5-HT$_{7A}$R membranes, 1 nM [^{3}H]-5-CT, and reference or test compounds were suspended in 0.25 mL of incubation buffer (50 mM Tris-HCl pH 7.4, 4 mM $MgCl_2$, 0.1%, ascorbic acid, 10 μM pargyline hydrochloride). The samples were incubated for 60 min at 37 °C. The incubation was stopped by rapid filtration, and the filters were washed with 3 × 0.25 mL of ice-cold buffer (50 mM Tris-HCl, pH 7.4). Nonspecific binding was determined in the presence of 10 μM 5-CT. Approximately 90% of specific binding was determined under these conditions. Concentrations required to inhibit 50% of radioligand specific binding (IC_{50}) were determined using six to nine different concentrations of the compound studied in two or three experiments with samples in

https://doi.org/10.1021/acschemneuro.1c00710
ACS Chem. Neurosci. XXXX, XXX, XXX−XXX

duplicate. Apparent inhibition constants (K_i) were determined by nonlinear curve fitting, using the Prism, version 5.0, GraphPad software.

Association Binding Assay. Constant affinity (k_{on}) of [^{3}H]-5-CT was assessed by association assay. The experiments were performed in MultiScreen plates (Merck Millipore) with glass fiber filters (GF/C), presoaked in 0.3% poly(ethylenimine) for 20 min. After this time, 130 μg of HEK-293-5-HT$_{7A}$R membranes and 1 nM [^{3}H]-5-CT were suspended in 0.25 mL of incubation buffer (see above). The samples were incubated at 37 °C for a range of time points (0, 5, 10, 15, 20, 30, 60, 90 min). The incubation was stopped by rapid filtration and the filters were washed with 3 × 0.25 mL of ice-cold buffer (50 mM Tris-HCl, pH 7.4). Constant affinity (k_{on}) value was determined by nonlinear curve fitting, using the Prism, version 5.0, GraphPad software.

Dissociation Binding Assay. The dissociation rate (k_{off}) of [^{3}H]-5CT was assessed by dissociation assay. The experiment was performed in MultiScreen plates (Merck Millipore) with glass fiber filters (GF/C), presoaked in 0.3% poly(ethylenimine) for 20 min. After this time, 130 μg of HEK-293-5-HT$_{7A}$R membranes and 1 nM [^{3}H]-5-CT were suspended in a 0.25 mL of incubation buffer (see above) at 37 °C for 30 min. After this equilibrium time, 10 μM 5-CT was added and the dissociation was initiated at a range of time points (90, 60, 30, 20, 15, 10, 5, 0 min). The incubation was stopped by rapid filtration and the filters were washed with 3 × 0.25 mL of ice-cold buffer (50 mM Tris-HCl, pH 7.4). Dissociation rate (k_{off}) value was determined by nonlinear curve fitting, using the Prism, version 5.0, GraphPad software.

Competition Association Assay. To determine the k_{on} and k_{off} values of selected ligands, all compounds were tested at their respective K_i. The experiments were performed in MultiScreen plates (Merck Millipore) with glass fiber filters (GF/C), presoaked in 0.3% poly(ethylenimine) for 20 min. After this time, 130 μg of HEK-293-5-HT$_{7A}$R membranes, 1 nM [^{3}H]-5CT, and reference or test compounds at their K_i concentration were suspended in 0.25 mL of incubation buffer (see above). The samples were incubated at 37 °C for a range of time points (0, 5, 10, 15, 20, 30, 60, 90 min). The incubation was stopped by rapid filtration, and the filters were washed with 3 × 0.25 mL of ice-cold buffer (50 mM Tris-HCl, pH 7.4). The k_{on} and k_{off} values were determined by nonlinear curve fitting, using the Prism, version 5.0, GraphPad software.

Lipophilicity Index. Lipophilicity indices were measured by a reversed-phase HPLC method consisting of an Agilent 1260 Infinity Binary LC system equipped with a diode array detector (Open Lab software was used to analyze the chromatographic data) under isocratic conditions. The capacity factors (k') were measured with a Phenomenex Gemini C18 (250 × 4.6 mm, 5 μm particle size) as nonpolar stationary phase and with MeOH/0.01 M phosphate buffer pH 7.4 (7:3 v/v) as mobile phase. This mobile phase composition was chosen for the analysis due to reasonable retention times for all compounds analyzed. All compounds were dissolved in methanol (0.1 mg/mL), injection volumes were 10 μL, the flow rate was 1 mL/min, and the detection was performed at λ = 230 and 254 nm. Retention times (t_R) were measured at least from three separate injections, and dead time (t_0) was measured as the solvent front. For each compound, the average retention time (t_R) of three consecutive injections was used to calculate the log k' values ($\log k' = \log[(t_R - t_0)/t_0]$).

Computational Studies. *Descriptor Calculation.* Molecular descriptors were calculated using the recently developed Mordred package.[56] The correlations of molecular descriptor values with compound residence times were determined using the scikit-learn package.[57]

Docking and MD Simulation. 5-HT$_7$R homology models were prepared using the crystal structure of 5-HT$_{1B}$R (PDBID: 4IAR) as a template and Modeller software as previously reported.[48] The preparation of compounds (generation of three-dimensional conformations and protonation states at pH 7.4) was performed using LigPrep[58] from the Schrödinger Suite, and docking of compounds (extra precision mode) was performed using Glide from the same software package.[59] The MD simulations were carried out using Schrödinger's Desmond software[60] for each of the obtained ligand−receptor complexes (duration time = 1000 ns; TIP3P as the solvent model and POPC (palmitoyl-oleil-phosphatidylcoline) as the membrane model were used).[61]

Neurite Outgrowth in Mouse Neuronal Primary Cultures. *Neuronal Primary Cultures.* C57BL/6 mice were housed and sacrificed in accordance with the recommendations of the European Commission (EU Directive 2010/63/EU for animal experiments). The animals were bred in-house at the Institute of Genetics and Biophysics "Adriano Buzzati Traverso", CNR, Naples, Italy. All of the procedures related to animal treatments were approved by Ethic-Scientific Committee for Animal Experiments. Primary cultures were prepared from WT C57BL/6J mouse pups at the postnatal day 1 (P1) or postnatal day 3 (P3). Pups of both sexes were used. The mice brains were quickly isolated from pups under sterile conditions and placed in HBSS (Cat. No. 24020-091; Thermo Fisher Scientific, Milan, Italy). The areas of interest, striatum (STR), cortex (CTX), and hippocampus (HPP), were dissected from the brain under a stereomicroscope in HBSS with 10% fetal bovine serum (FBS, Euroclone, Milan, Italy) and then placed in HBSS w/o serum. The collected tissues were enzymatically dissociated by incubation for 90 s at 37 °C in a trypsin solution (0.1% trypsin in HBSS, Sigma, Milan Italy) containing 0.01% pancreatic DNAse (Sigma, Milan Italy). Enzymatic dissociation was blocked replacing the medium with HBSS containing Ca^{2+}/Mg^{2+} and 10% fetal bovine serum (FBS) medium. The cells were washed in HBSS Ca^{2+}/Mg^{2+} and mechanically dissociated by pipetting 10 times in 1 mL of Neurobasal A medium (NBM-A) containing 0.01% DNase. After 5 min of centrifugation at 500 rpm, the cells were resuspended in 1 mL of NBM-A, and their concentration was determined on the basis of the total cell count after the trypan blue dye exclusion. Dissociated cells were plated in NBM-A medium supplemented with B27 (Thermo Fisher Scientific) and 5% FBS, 2 mM Glutamax (Thermo Fisher Scientific), 50 U/mL penicillin, and 50 mg/mL streptomycin (Thermo Fisher Scientific) at a density of 35 × 103/cm^2 onto sterilized 12 mm coverslips (Corning Optical Communications S.r.l., Torino, Italy) freshly coated with 15 μg/mL of poly-D-lysine (Sigma-Aldrich, Milan, Italy). After 1 day, in vitro (DIV) FBS was withdrawn and every third DIV, half of the medium was replaced by fresh medium without FBS. Cultures were maintained at 37 °C and 5% CO_2 in a humidified incubator for 3−4 days. Each experimental point was performed from three independent cell preparations, and each neuronal culture was technically replicated three times.

Drugs and Reagents. The cell cultures were treated with the agonists LP-211(100 nM) and **4** (100 nM), the 5-HT$_7$R antagonist SB-269970 (100 nM) (Tocris, Milan, Italy), or with a combination of these drugs. Drugs were added to cultures at DIV indicated in the Results and Discussion section or in the figure legends and incubated for an appropriate time.

Immunofluorescence and Morphological Analyses. For morphological analyses, postnatal cultures were fixed in 4% paraformaldehyde in phosphate-buffered saline (PBS) for 20 min at residence time (RT), washed three times in PBS, and stored at −20 °C in PBS/glycerol (1:1 v/v) until use. After removal of the PBS/glycerol medium, the cells were washed three times in PBS and permeabilized for 15 min in PBS containing 0.1% Triton-X-100. The neurons were treated for 30 min at RT in blocking solution (3% bovine serum albumin (BSA) in PBS) and then incubated overnight at 4 °C with the primary antibody in PBS containing 1% BSA. The monoclonal antibody against neuron-specific class III ß-tubulin (Tuj1; Sigma-Aldrich T8660, 1:750) was used to stain neurons. The cells were then washed in PBS and incubated for 2 h at RT with fluorescent-labeled secondary antibodies (Alexa Fluor 594, 1:400; ThermoFisher Scientific) in PBS with 1% BSA. After washing, the cells were stained with 40,6-diamidino-2-phenylindole (DAPI; nuclear stain, 1:1000) for 10 min at 22 °C and mounted on a coverslip with an oil mounting solution (Mowiol, Sigma-Aldrich). To evaluate neurite length, fluorescent signals from Tuj1 stained neurons were detected with a microscope (Leica DM6000B, Wetzlar, Germany) equipped with a

https://doi.org/10.1021/acschemneuro.1c00710
ACS Chem. Neurosci. XXXX, XXX, XXX−XXX

20× objective. Images were acquired with a high-resolution camera using the software Leica Application Suite and analyzed by the image processing software ImageJ (https://imagej.net/Welcome). The length of neurites was measured as previously described.[18] A total of 10−15 fields for each cell culture condition was used from at least three independent culture wells. The analyses were carried out "blind" to avoid any subjective influences during measurements.

■ ASSOCIATED CONTENT

Supporting Information

The Supporting Information is available free of charge at https://pubs.acs.org/doi/10.1021/acschemneuro.1c00710.

Synthetic schemes and procedures of compounds **2**, **3**, and **11**; correlation plot between residence time and pK_i and between residence time and log k'; correlation analysis of molecular descriptors and residence time; ligand−protein interaction patterns obtained for the active and inactive forms of 5-HT_7R; results of MD simulations for active 5-HT_7R; RMSD of ligands during MD simulations; ligand−protein interaction patterns obtained during MD simulations for inactive 5-HT_7R; analysis of the distance between Cα of W23 × 50 and L2 × 65 during MD; analysis of C_α-C_β-C_γ of W23 × 50 during MD; interaction patterns with W23×50 obtained during MD; and ligand−protein interaction patterns obtained during MD simulations for selected ECL2 residues (PDF)

■ AUTHOR INFORMATION

Corresponding Author

Enza Lacivita − *Dipartimento di Farmacia-Scienze del Farmaco, Università degli Studi di Bari Aldo Moro, 70125 Bari, Italy;* orcid.org/0000-0003-2443-1174; Email: enza.lacivita@uniba.it

Authors

Eduardo Penna − *Department of Biology, University of Naples Federico II, 80126 Naples, Italy; Biofordrug srl, 70019 Triggiano (Bari), Italy*

Mauro Niso − *Dipartimento di Farmacia-Scienze del Farmaco, Università degli Studi di Bari Aldo Moro, 70125 Bari, Italy*

Sabina Podlewska − *Maj Institute of Pharmacology, Polish Academy of Sciences, 31-343 Kraków, Poland;* orcid.org/0000-0002-2891-5603

Floriana Volpicelli − *Department of Biology, University of Naples Federico II, 80126 Naples, Italy*

Marianna Crispino − *Department of Biology, University of Naples Federico II, 80126 Naples, Italy*

Carla Perrone-Capano − *Department of Pharmacy, School of Medicine and Surgery, University of Naples Federico II, 80131 Naples, Italy; Institute of Genetics and Biophysics "Adriano Buzzati Traverso", National Research Council (CNR), 80131 Naples, Italy*

Andrzej J. Bojarski − *Maj Institute of Pharmacology, Polish Academy of Sciences, 31-343 Kraków, Poland;* orcid.org/0000-0003-1417-6333

Marcello Leopoldo − *Dipartimento di Farmacia-Scienze del Farmaco, Università degli Studi di Bari Aldo Moro, 70125 Bari, Italy;* orcid.org/0000-0001-8401-2815

Complete contact information is available at: https://pubs.acs.org/10.1021/acschemneuro.1c00710

Author Contributions

[▽]E.P. and S.P. contributed equally to this work. The manuscript was written through contributions of all authors. All authors have given approval to the final version of the manuscript.

Funding

This work was supported by (1) "Finanziamento Ricerca di Ateneo" by Università degli Studi di Bari; (2) POR Campania FESR 2014/2020 (Project N. B61G18000470007) from Regione Campania, (3) Industrial PhD fellowship (n. DOT1318787) PON-RI 2014-2020, and (4) Progetto Dipartimentale 000005-2020 and Progetto http://000005_2018_rare.plat.net/

Notes

The authors declare no competing financial interest.

■ ACKNOWLEDGMENTS

S.P., A.J.B., E.L., and M.L. are members of the COST Action CA 18133 "European Research Network on Signal Transduction—ERNEST".

■ ABBREVIATIONS USED

CPM, counts per minute; CTRL, control; ECL, extracellular loop; GPCRs, G protein-coupled receptors; IFD, induced-fit docking; LSD, lysergic acid diethylamide; MD, molecular dynamics; RT, residence time; SKRs, structure−kinetics relationships

■ REFERENCES

(1) Guo, D.; Hillger, J. M.; IJzerman, A. P.; Heitman, L. H. Drug-target residence time − a case for G protein-coupled receptors. *Med. Res. Rev.* **2014**, *34*, 856−892.

(2) Copeland, R. A. The drug-target residence time model: a 10-year retrospective. *Nat. Rev. Drug Discov.* **2016**, *15*, 87−95.

(3) Sykes, D. A.; Moore, H.; Stott, L.; Holliday, N.; Javitch, J. A.; Lane, J. R.; Charlton, S. J. Extrapyramidal side effects of antipsychotics are linked to their association kinetics at dopamine D-2 receptors. *Nat. Commun.* **2017**, *8*, No. 763.

(4) de Witte, W. E. A.; Danhof, M.; van der Graaf, P. H.; de Lange, E. C. M. In vivo target residence time and kinetic selectivity: the association rate constant as determinant. *Trends Pharmacol. Sci.* **2016**, *37*, 831−842.

(5) Hoffmann, C.; Castro, M.; Rinken, A.; Leurs, R.; Hill, S. J.; Vischer, H. F. Ligand residence time at G-protein coupled receptors − why we should take our time to study it. *Mol. Pharmacol.* **2015**, *88*, 552−560.

(6) Dahl, G.; Akerud, T. Pharmacokinetics and the drug target residence time concept. *Drug Discovery Today* **2013**, *18*, 697−707.

(7) Hothersall, J. D.; Brown, A. J.; Dale, I.; Rawlins, P. Can residence time offer a useful strategy to target agonist drugs for sustained GPCR responses? *Drug Discovery Today* **2016**, *21*, 90−96.

(8) Núñez, S.; Venhorst, J.; Kruse, C. G. Target-drug interactions: first principles and their application to drug discovery. *Drug Discovery Today* **2012**, *17*, 10−22.

(9) Swinney, D. C. The role of binding kinetics in therapeutically useful drug action. *Curr. Opin. Drug Discovery Dev.* **2009**, *12*, 31−39.

(10) Dowling, M. R.; Charlton, S. J. Quantifying the association and dissociation rates of unlabelled antagonists at muscrinic M_3 receptor. *Br. J. Pharmacol.* **2006**, *148*, 927−937.

(11) Kapur, S.; Seeman, P. Antipsychotic agents differ in how fast they come off the dopamine D2 receptors. Implication for atypical antipsychotic action. *J. Psychiatr. Neurosci.* **2000**, *25*, 161−166.

(12) Schuetz, D. A.; de Witte, W. E. A.; Wong, Y. C.; Knasmueller, B.; Richter, L.; Kokh, D. B.; Sadiq, S. K.; Bosma, R.; Nederpelt, I.; Heitman, L. H.; Segala, E.; Amaral, M.; Guo, D.; Andres, D.; Georgi,

V.; Stoddart, L. A.; Hill, S. J.; Cooke, R. M.; de Graaf, C.; Leurs, R.; Frech, M.; Wade, R. C.; de Lange, E. C. M.; IJzerman, A. P.; Müller-Fahrnow, A.; Ecker, G. F. Kinetics for drug-discovery: an industry-driven effort to target drug residence time. *Drug Discovery Today* **2017**, *22*, 896−911.

(13) Santos, R.; Ursu, O.; Gaulton, A.; Bento, A. P.; Donadi, R. S.; Bologa, C. G.; Karlsson, A.; Al-Lazikani, B.; Hersey, A.; Oprea, T. I.; Overington, J. P. A comprehensive map of molecular drug targets. *Nat. Rev. Drug Discovery* **2017**, *16*, 19−34.

(14) Modica, M. N.; Lacivita, E.; Intagliata, S.; Salerno, L.; Romeo, G.; Pittalà, V.; Leopoldo, M. Structure-activity relationships and therapeutic potentials of 5-HT$_7$ receptor ligands: an update. *J. Med. Chem.* **2018**, *61*, 8475−8503.

(15) Nikiforuk, A. Targeting the serotonin 5-HT$_7$ receptor in the search for treatments for CNS disorders: rationale and progress to date. *CNS Drugs* **2015**, *29*, 265−275.

(16) Kobe, F.; Guseva, D.; Jensen, T. P.; Wirth, A.; Renner, U.; Hess, D.; Muller, M.; Medrihan, L.; Zhang, W.; Zhang, M.; Braun, K.; Westerholz, S.; Herzog, A.; Radyushkin, K.; El-Kordi, A.; Ehrenreich, H.; Richter, D. W.; Rusakov, D. A.; Ponimaskin, E. 5-HT7R/G12 signaling regulates neuronal morphology and function in an age-dependent manner. *J. Neurosci.* **2012**, *32*, 2915−2930.

(17) Speranza, L.; Chambery, A.; Di Domenico, M.; Crispino, M.; Severino, V.; Volpicelli, F.; Leopoldo, M.; Bellenchi, G. C.; di Porzio, U.; Perrone-Capano, C. The serotonin receptor 7 promotes neurite outgrowth via ERK and Cdk5 signaling pathways. *Neuropharmacology* **2013**, *67*, 155−167.

(18) Speranza, L.; Giuliano, T.; Volpicelli, F.; De Stefano, M. E.; Lombardi, L.; Chambery, A.; Lacivita, E.; Leopoldo, M.; Bellenchi, G. C.; di Porzio, U.; Crispino, M.; Perrone-Capano, C. Activation of 5-HT7 receptor stimulates neurite elongation through mTOR, Cdc42 and actin filaments dynamics. *Front. Behav. Neurosci.* **2015**, *9*, No. 62.

(19) Speranza, L.; Labus, J.; Volpicelli, F.; Guseva, D.; Lacivita, E.; Leopoldo, M.; Bellenchi, G. C.; di Porzio, U.; Bijata, M.; Perrone-Capano, C.; Ponimaskin, E. Serotonin 5-HT7 receptor increases the density of dendritic spines and facilitates synaptogenesis in forebrain neurons. *J. Neurochem.* **2017**, *141*, 647−661.

(20) Costa, L.; Spatuzza, M.; D'Antoni, S.; Bonaccorso, C. M.; Trovato, C.; Musumeci, S. A.; Leopoldo, M.; Lacivita, E.; Catania, M. V.; Ciranna, L. Activation of 5-HT7 serotonin receptors reverses metabotropic glutamate receptor-mediated synaptic plasticity in wild-type and Fmr1 knockout mice, a model of Fragile X syndrome. *Biol. Psychiatry* **2012**, *72*, 924−933.

(21) Costa, L.; Sardone, L. M.; Bonaccorso, C. M.; D'Antoni, S.; Spatuzza, M.; Gulisano, W.; Tropea, M. R.; Puzzo, D.; Leopoldo, M.; Lacivita, E.; Catania, M. V.; Ciranna, L. Activation of serotonin 5-HT$_7$ receptors modulates hippocampal synaptic plasticity by stimulation of adenylate cyclases and rescues learning and behavior in a mouse model of Fragile X syndrome. *Front. Mol. Neurosci.* **2018**, *11*, No. 353.

(22) De Filippis, B.; Nativio, P.; Fabbri, A.; Ricceri, L.; Adriani, W.; Lacivita, E.; Leopoldo, M.; Passarelli, F.; Fuso, A.; Laviola, G. Pharmacological stimulation of the brain serotonin receptor 7 as a novel therapeutic approach for Rett syndrome. *Neuropsychopharmacology* **2014**, *39*, 2506−2518.

(23) Valenti, D.; de Bari, L.; Vigli, D.; Lacivita, E.; Leopoldo, M.; Laviola, G.; Vacca, R. A.; De Filippis, B. Stimulation of the brain serotonin receptor 7 rescues mitochondrial dysfunction in female mice from two models of Rett syndrome. *Neuropharmacology* **2017**, *121*, 79−88.

(24) Hedlund, P. B.; Leopoldo, M.; Caccia, S.; Sarkisyan, G.; Fracasso, C.; Martelli, G.; Lacivita, E.; Berardi, F.; Perrone, R. LP-211 is a brain penetrant selective agonist for the serotonin 5-HT(7) receptor. *Neurosci. Lett.* **2010**, *481*, 12−16.

(25) Sykes, D. A.; Stoddart, L. A.; Kilpatrick, L. E.; Hill, S. J. Binding Kinetics of ligands acting at GPCRs. *Mol. Cell. Endocrinol.* **2019**, *485*, 9−19.

(26) Satała, G.; Duszyńska, B.; Lenda, T.; Nowak, G.; Bojarski, A. J. Allosteric Inhibition of Serotonin 5-HT$_7$ Receptors by Zinc Ions. *Mol. Neurobiol.* **2018**, *55*, 2897−2910.

(27) Armstrong, J. L.; Casey, A. B.; Saraf, T. S.; Mukherjee, M.; Booth, R. G.; Canal, C. E. (S)-5-(2′-Fluorophenyl)-N,N-dimethyl-1,2,3,4-tetrahydronaphthalen-2-amine, a Serotonin Receptor Modulator, Possesses Anticonvulsant, Prosocial, and Anxiolytic-like Properties in an Fmr1 Knockout Mouse Model of Fragile X Syndrome and Autism Spectrum Disorder. *ACS Pharmacol. Transl. Sci.* **2020**, *3*, 509−523.

(28) Motulsky, H. J.; Mahan, L. C. The kinetics of competitive radioligand binding predicted by the law of mass action. *Mol. Pharmacol.* **1984**, *25*, 1−9.

(29) Pan, A. C.; Borhani, D. W.; Dror, R. O.; Shaw, D. E. Molecular determinants of drug-receptor binding kinetics. *Drug Discovery Today* **2013**, *18*, 667−673.

(30) Tresadern, G.; Bartolome, J. M.; Macdonald, G. J.; Langlois, X. Molecular properties affecting fast dissociation from D2 receptor. *Bioorg. Med. Chem.* **2011**, *19*, 2231−2241.

(31) Vilums, M.; Zweemer, A. J.; Barmare, F.; van der Gracht, A. M.; Bleeker, D. C.; Yu, Z.; de Vries, H.; Gross, R.; Clemens, J.; Krenitsky, P.; Brussee, J.; Stamos, D.; Saunders, J.; Heitman, L. H.; IJzerman, A. P. When structure-affinity relationships meet structure-kinetics relationships: 3-((inden-1-yl)amino)-1-isopropyl-cyclopentane-1-carboxamides as CCR2 antagonists. *Eur. J. Med. Chem.* **2015**, *93*, 121−134.

(32) Soethoudt, M.; Hoorens, M. W. H.; Doelman, W.; Martella, A.; van der Stelt, M.; Heitman, L. H. Structure-kinetic relationship studies of cannabinoid CB2 receptor agonists reveal substituent-specific lipophilic effects on residence time. *Biochem. Pharmacol.* **2018**, *152*, 129−142.

(33) Hansen, H. D.; Lacivita, E.; Di Pilato, P.; Herth, M. M.; Lehel, S.; Ettrup, A.; Andersen, V. L.; Dyssegaard, A.; De Giorgio, P.; Perrone, R.; Berardi, F.; Colabufo, N. A.; Niso, M.; Knudsen, G. M.; Leopoldo, M. Synthesis, radiolabeling and in vivo evaluation of [(11)C](R)-1-[4-[2-(4-methoxyphenyl)phenyl]piperazin-1-yl]-3-(2-pyrazinyloxy)-2-propanol, a potential PET radioligand for the 5-HT(7) receptor. *Eur. J. Med. Chem.* **2014**, *79*, 152−163.

(34) Lacivita, E.; Niso, M.; Stama, M. L.; Arzuaga, A.; Altamura, C.; Costa, L.; Desaphy, J. F.; Ragozzino, M. E.; Ciranna, L.; Leopoldo, M. Privileged scaffold-based design to identify a novel drug-like 5-HT7 receptor-preferring agonist to target Fragile X syndrome. *Eur. J. Med. Chem.* **2020**, *199*, No. 112395.

(35) Sykes, D. A.; Charlton, S. J. Slow receptor dissociation is not a key factor in the duration of action of inhaled long-acting ss(2)-adrenoceptor agonists. *Br. J. Pharmacol.* **2012**, *165*, 2672−2683.

(36) Yu, Z.; van Veldhoven, J. P. D.; Louvel, J.; Hart, I. M. E.; Rook, M. B.; van der Heyden, M. A. G.; Heitman, L. H.; Ijzerman, A. P. Structure-affinity relationships (SARs) and structure-kinetics relationships (SKRs) of K(v)11.1 blockers. *J. Med. Chem.* **2015**, *58*, 5916−5929.

(37) Liu, C.; Xia, L.; Fu, K.; Cao, X.; Yan, W.; Cheng, J.; Roux, T.; Peletier, L. A.; Yin, X.; Guo, D. Revisit ligand-receptor interaction at the human vasopressin V2 receptor: a kinetic perspective. *Eur. J. Pharmacol.* **2020**, *880*, No. 173157.

(38) Tautermann, C. S. Impact, determination and prediction of drug-receptor residence times for GPCRs. *Curr. Opin. Pharmacol.* **2016**, *30*, 22−26.

(39) Bosma, R.; Wang, Z.; Kooistra, A. J.; Bushby, N.; Kuhne, S.; van den Bor, J.; Waring, M. J.; de Graaf, C.; de Esch, I. J.; Vischer, H. F.; Sheppard, R. J.; Wijtmans, M.; Leurs, R. Route to prolonged residence time at the histamine H1 receptor: growing from desloratadine to rupatadine. *J. Med. Chem.* **2019**, *62*, 6630−6644.

(40) Ganotra, G. K.; Wade, R. C. Prediction of drug-target binding kinetics by comparative binding energy analysis. *ACS Med. Chem. Lett.* **2018**, *9*, 1134−1139.

(41) Qu, S.; Huang, S.; Pan, X.; Yang, L.; Mei, H. Constructing interconsistent, reasonable, and predictive models for both the kinetic and thermodynamic properties of HIV-1 protease inhibitors. *J. Chem. Inf. Model.* **2016**, *56*, 2061−2068.

https://doi.org/10.1021/acschemneuro.1c00710
ACS Chem. Neurosci. XXXX, XXX, XXX−XXX

(42) Chiu, S. H.; Xie, L. Toward high-throughput predictive modeling of protein binding/unbinding kinetics. *J. Chem. Inf. Model.* **2016**, *56*, 1164−1174.

(43) Xia, L.; Burger, W. A. C.; van Veldhoven, J. P. D.; Kuiper, B. J.; van Duijl, T. T.; Lenselink, E. B.; Paasman, E.; Heitman, L. H.; IJzerman, A. P. Structure−affinity relationships and structure−kinetics relationships of pyrido[2,1-f]purine-2,4-dione derivatives as human adenosine A_3 receptor antagonists. *J. Med. Chem.* **2017**, *60*, 7555−7568.

(44) Prinz, J. H.; Wu, H.; Sarich, M.; Keller, B.; Senne, M.; Held, M.; Chodera, J. D.; Schutte, C.; Noé, F. Markov models of molecular kinetics: generation and validation. *J. Chem. Phys.* **2011**, *134*, No. 174105.

(45) Tang, Z.; Chang, C. A. Energy barriers, molecular motions, and residence time in ligand dissociation: a computational study on type II inhibitors binding to CDK8/CycC. *BioRxiv* **2017**, *7*, 1−24.

(46) Tiwary, P.; Limongelli, V.; Salvalaglio, M.; Parrinello, M. Kinetics of protein-ligand unbinding: Predicting pathways, rates, and rate-limiting steps. *Proc. Natl. Acad. Sci. U.S.A.* **2015**, *112*, E386−E391.

(47) Maragliano, L.; Vanden-Eijnden, E. A. Temperature accelerated method for sampling free energy and determining reaction pathways in rare events simulations. *Chem. Phys. Lett.* **2006**, *426*, 168−175.

(48) Rataj, K.; Witek, J.; Mordalski, S.; Kosciolek, T.; Bojarski, A. J. Impact of template choice on homology model efficiency in virtual Sscreening. *J. Chem. Inf. Model.* **2014**, *54*, 1661−1668.

(49) Pándy-Szekeres, G.; Munk, C.; Tsonkov, T. M.; Mordalski, S.; Harpsøe, K.; Hauser, A. S.; Bojarski, A. J.; Gloriam, D. E. GPCRdb in 2018: adding GPCR structure models and ligands. *Nucleic Acids Res.* **2018**, *46*, D440−D446.

(50) Wacker, D.; Wang, S.; McCorvy, J. D.; Betz, R. M.; Venkatakrishnan, A. J.; Levit, A.; lansu, K.; Schools, Z. L.; Che, T.; Nichols, D. E.; Shoichet, B. K.; Dror, R. O.; Roth, B. L. Crystal Structure of an LSD-Bound Human serotonin receptor. *Cell* **2017**, *168*, 377−389.

(51) McCorvy, J. D.; Butler, K. V.; Kelly, B.; Rechsteiner, K.; Karpiak, J.; Betz, R. M.; Kormos, B. L.; Shochet, B. K.; Dror, R. O.; Jin, J.; Roth, B. L. Structure-inspired design of β-arrestin-biased ligands for aminergic GPCRs. *Nat. Chem. Biol.* **2018**, *14*, 126−134.

(52) Wang, S.; Che, T.; Levit, A.; Shoichet, B. K.; Wacker, D.; Roth, B. L. Structure of the D2 dopamine receptor bound to the atypical antipsychotic drug risperidone. *Nature* **2018**, *555*, 269−273.

(53) Ågren, R.; Zeberg, H.; Stępniewski, T. M.; Free, R. B.; Reilly, S. W.; Luedtke, R. R.; Århem, P.; Ciruela, F.; Sibley, D. R.; Mach, R. H.; Selent, J.; Nilsson, J.; Sahlholm K, K. Ligand with Two Modes of Interaction with the Dopamine D2 Receptor-An Induced-Fit Mechanism of Insurmountable Antagonism. *ACS Chem. Neurosci.* **2020**, *11*, 3130−3143.

(54) Volpicelli, F.; Speranza, L.; Pulcrano, S.; De Gregorio, R.; Crispino, M.; De Sanctis, C.; Leopoldo, M.; Lacivita, E.; di Porzio, U.; Bellenchi, G. C.; Perrone-Capano, C. The microRNA-29a modulates serotonin 5-HT_7 receptor expression and its effects on hippocampal neuronal morphology. *Mol. Neurobiol.* **2019**, *56*, 8617−8627.

(55) Lacivita, E.; Niso, M.; Hansen, H. D.; Di Pilato, P.; Herth, M. M.; Lehel, S.; Ettrup, A.; Montenegro, L.; Perrone, R.; Berardi, F.; Colabufo, N. A.; Leopoldo, M.; Knudsen, G. M. Design, synthesis, radiolabeling and in vivo evaluation of potential positron emission tomography (PET) radioligands for brain imaging of the 5-HT_7 receptor. *Bioorg. Med. Chem.* **2014**, *22*, 1736−1750.

(56) Moriwaki, H.; Tian, Y. S.; Kawashita, N.; Takagi, T. Mordred: a molecular descriptor calculator. *J. Cheminform* **2018**, *10*, No. 4.

(57) Pedregosa, F.; Varoquaux, G.; Gramfort, A.; Michel, V.; Thirion, B.; Grisel, O.; Blondel, M.; Prettenhofer, P.; Weiss, R.; Dubourg, V.; Vanderplas, J.; Passos, A.; Cournapeau, D.; Brucher, M.; Perrot, M.; Duchesnay, E. Scikit-learn: Machine Learning in {P}ython. *J. Mach. Learn. Res.* **2011**, *12*, 2825−2830.

(58) *LigPrep, Schrödinger Release 2019-3*; LLC: New York, NY, 2019.

(59) *Glide, Schrödinger Release 2019-3*; LLC: New York, NY, 2019.

(60) Schrödinger Release 2019-3: Desmond Molecular Dynamics System, D. E. Shaw Research, New York, NY, 2019. *Maestro-Desmond Interoperability Tools*; Schrödinger: New York, NY, 2019.

(61) Jorgensen, W. L.; Chandrasekhar, J.; Madura, J. D.; Impey, R. W.; Klein, M. L. Comparison of simple potential functions for simulating liquid water. *J. Chem. Phys.* **1983**, *79*, 926−935.

https://doi.org/10.1021/acschemneuro.1c00710
ACS Chem. Neurosci. XXXX, XXX, XXX−XXX